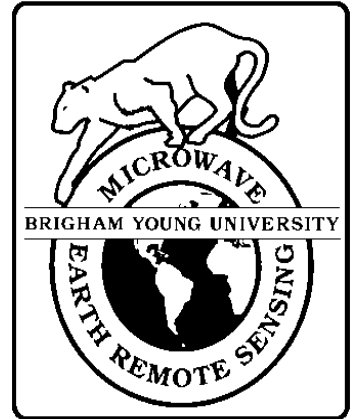




**Brigham Young University
Department of Electrical and
Computer Engineering**

**459 Clyde Building
Provo, Utah 84602**



Background and Accuracy Analysis of the Xfactor7 Table: Final Report on QuikScat X Factor Accuracy

**Brian E. Jones
David G. Long
Ivan S. Ashcraft
Arden T. Anderson**

13 January 1999

**MERS Technical Report # MERS 99-01
ECEN Department Report # TR-L120-99.1**

**Microwave Earth Remote Sensing (MERS)
Laboratory**

© Copyright 1999, Brigham Young University. All rights reserved.

Background and Accuracy Analysis of the Xfactor7 Table

Brian E. Jones, David G. Long, Ivan S. Ashcraft, Arden T. Anderson
Brigham Young University, Microwave Earth Remote Sensing Laboratory
459 CB, Provo, UT 84602 USA

January 13, 1999

Abstract

The SeaWinds instrument being developed by Jet Propulsion Laboratories (JPL) will be launched on QuikSCAT in spring 1999. SeaWinds will continue the retrieval of marine wind data by measuring and processing the normalized radar backscatter, σ_o . In order to speed up real time processing of σ_o , it was proposed to tabularize the X factor and the slice center locations pre-launch. The Xfactor7 code was developed to generate these tables and correct for attitude, orbit, and topography. We quantified the errors associated with the X Table generated by the Xfactor7 code. An extensive test has been completed for 16 evenly spaced orbit times with 100 different perturbations per beam per orbit time. The results show that the maximum error expected for the inner beam is 0.12 dB for X , 0.009 dB for X_{egg} , 0.024 degrees for the azimuth angle, and 0.008 for the elevation angle. For the outer beam the maximum errors are 0.05 dB for X , 0.012 dB for X_{egg} , 0.018 degrees for the azimuth angle, and 0.0045 degrees for the elevation angle.

1 Introduction

Space-borne retrieval of marine wind data is an increasingly important tool used in the study of the Earth's weather patterns. The SeaWinds instrument will continue the retrieval of wind data that was initiated by the NASA Scatterometer (NSCAT) mission. SeaWinds is being developed for launch on QuikSCAT in Spring 1999 and later on ADEOS-II in 2000. Brigham Young University (BYU) is working in conjunction with Jet Propulsion Laboratories (JPL) on the implementation of the X factor portion of the data retrieval code used with SeaWinds. This report will give a brief background on space-borne wind data retrieval, the motivation for the X table, and then an accuracy analysis of the X factor7 table.

2 Background for Wind Scatterometry

Winds give an insight to the weather patterns that effect our everyday lives. Because the Earth is mostly covered by water, a good understanding of marine winds would lead to a more accurate understanding and forecasting of the weather and other changes in the climate. Space-borne observance of the marine winds lends itself to more accurate coverage of the Earth than an Earth based observation station. A satellite can cover almost the entire Earth in one day whereas a land based station would only be able to cover a very small portion of the Earth.

When wind blows across the ocean, it causes the generation of very small surface waves, called capillary waves. These waves are on top of the much larger ocean waves. Scatterometers can be used to measure the amount of backscatter off the ocean surface. The stronger the wind is, the rougher the ocean surface will be, thus more energy will be returned to the scatterometer. If no wind is present then no energy will be backscattered because it will all be reflected. The normalized radar backscatter, σ_o , is a measure of this returned energy. It is related to the power transmitted and backscattered by the radar equation,

$$P_s = \frac{P_t G^2 \lambda^2 A}{(4\pi)^3 R^4} \sigma_o \quad (1)$$

where P_t is the power transmitted, P_s is the power backscattered, G is the gain of the transmitting antenna, λ is the wavelength of the electromagnetic wave, A is the effective illuminated area, and R is the distance from the scatterometer to the target. Because the power returned, P_r , is a sum of the power backscattered, P_s , and the noise power, P_N , the noise term must be subtracted from P_r to get P_s . Equation (1) is only an approximation for σ_o . A more exact equation for σ_o is

$$P_s = \frac{\lambda^2}{(4\pi)^3} \int_{area} \frac{P_t G^2 \sigma_o}{R^4} dA, \quad (2)$$

where the area is the illuminated area. Assuming σ_o is constant over the footprint, we relate the normalized radar backscatter to P_s in terms of a radar calibration parameter, X ,

$$\sigma_o = \frac{P_s}{X} \quad (3)$$

where X is defined as

$$X = \frac{\lambda^2}{(4\pi)^3} \int_{area} \frac{P_t G^2}{R^4} dA. \quad (4)$$

In order to find the wind speed and direction at a specific point on the ocean multiple measurements of σ_o must be made.

3 Motivation for the X Table

3.1 X Factor Tabularization

SeaWinds has a rotating parabolic dish antenna (see Fig. 1). It uses a dual ‘‘pencil-beam’’ system which is a departure from the previous ‘‘fan-beam’’ system used by NSCAT and other space-borne scatterometers. The resulting antenna pattern is elliptical (see Fig. 2) instead of rectangular. There is an inner beam footprint and an outer beam footprint. In order to achieve higher resolution, the ‘egg’ is divided up into 12 ‘slices’ for both beams using transmit modulation and signal processing, as can be seen in Fig. 3. σ_o is then calculated for each slice.

SeaWind’s antenna radiates pulses at 13.4 GHz across Earth’s surface, making around 400,000 measurements a day. It is able to cover approximately 90% of Earth’s surface in one day. Because of the enormity of the measurements taken, it was necessary to find ways to decrease the processing time for computing σ_o . To compute X it is necessary to evaluate an integral [Eq.(4)] which is very time consuming in real-time processing. It has been proposed to tabularize X for every orbit time¹ and azimuth angle², before the launch of SeaWinds, to accelerate the processing.

Two parts of the X Table deal with the X factor: the table of nominal X values and the coefficients A, B, C , and D that are used to account for attitude and orbit perturbations. The nominal case is when there are no perturbations, i.e. the satellite is at the expected point in the orbit with perfect attitude (the roll, pitch, and yaw of the satellite) and the orbit parameters of eccentricity and argument of perigee are equal to the nominal values. When the satellite is in orbit, the X Table needs to account for perturbations, i.e. when the satellite deviates from the nominal orbit or attitude. This leads to the X equation

$$X = X_{nom} + A + B \cdot \Delta f + C \cdot \Delta f^2 + D \cdot \Delta f^3 \quad (5)$$

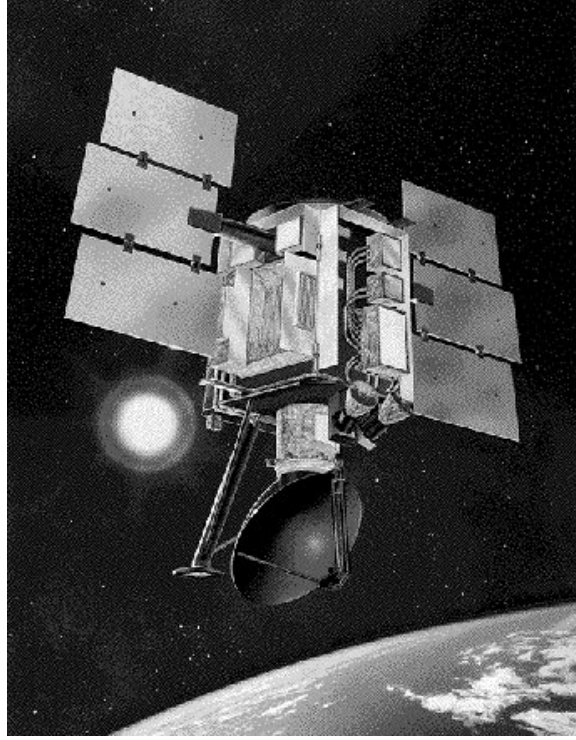
where Δf is the baseband frequency shift (in frequency bins) caused by perturbations in the orbit and attitude, and error in the Doppler tracking.

Δf is found by taking the difference between the baseband frequency at the bore-sight

¹Orbit time is the satellite position relative to Earth. For SeaWinds, it is defined as the time in seconds from the ascending node. Orbit time 0 is at the equator, 1515 at the North pole, 3030 at the equator again, 4545 at the South pole, and 6060 at the equator again

²Azimuth angle(Φ) is the angle the antenna is rotated relative to its reference position (from 0 to 360 degrees) at right angles to the satellite velocity vector on the left side of the satellite as viewed from above.

Figure 1: SeaWinds on QuikSCAT



for the nominal case³ and the baseband frequency at the bore-sight for the perturbed case, adding the error in Doppler tracking, and then converting the result to frequency bins:

$$\Delta f = (f_{nom} - f_{pert} + f_{err}) \cdot T \cdot N_{FFT}. \quad (6)$$

T is the sample time in seconds, and N_{FFT} is the number of points in the FFT. The equations for obtaining f_{nom} and f_{pert} are

$$f_{nom} = fd_{nom} + R_{constant} \cdot r_{nom} \quad (7)$$

and

$$f_{pert} = fd_{pert} + R_{constant} \cdot r_{pert}. \quad (8)$$

The variable fd is Doppler frequency shift for point the corresponding to the electrical bore-sight for the nominal and perturbed cases respectively and r is the slant range to the same point.

The elevation angle (Θ) electrical bore-sight currently being used by BYU is 39.85° for the inner beam and 45.95° for the outer beam. The azimuth angle (Φ) electrical bore-sight is halfway between the transmit pulse and receive pulse, offset by 0.15° .

To account for the effects of the aforementioned perturbations, X is calculated for 50 different combinations of perturbations. A plot of X vs. Δf can be seen in Fig. 4 (a). A , B , C , and D are calculated by using a third order polynomial fit for this set of points as

Figure 2: Antenna pattern for SeaWinds

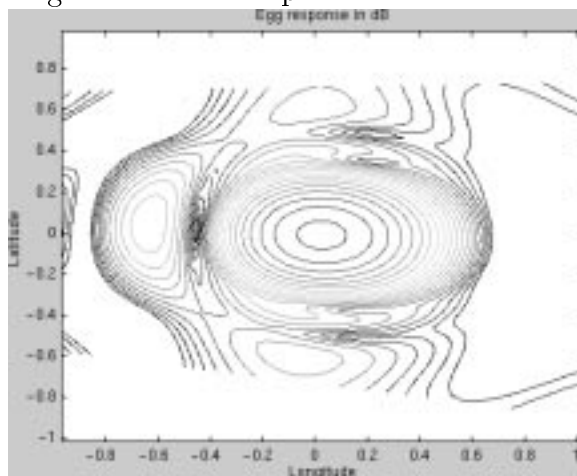
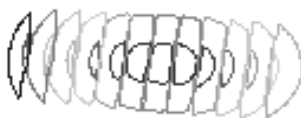


Figure 3: 12 slices of the 'egg'



given in Eq. (5).

When the X Table is generated, the coefficients are generated for a specified range of orbit times and azimuth angles. Then for a specific orbit and azimuth time, the coefficients are interpolated from the X Table and X can be calculated by plugging in the computed Δf . This will accelerate data processing because the X Table can be generated before SeaWinds is launched.

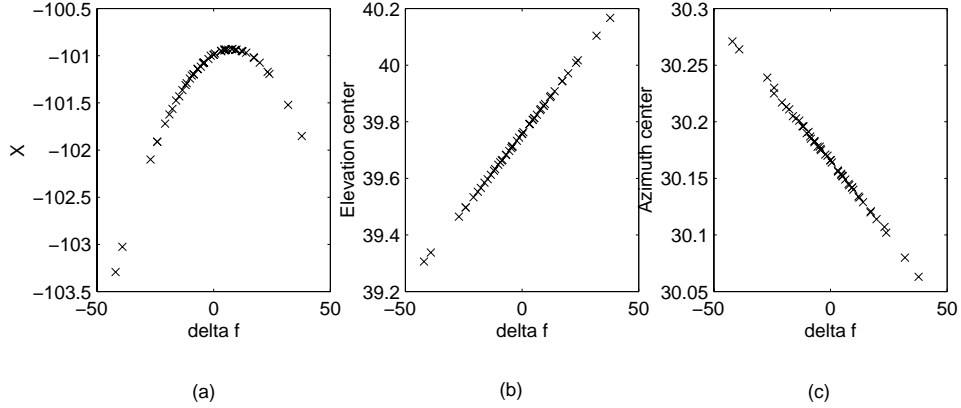
3.2 Slice Center Location Tabularization

Another part of the X Table is for the location of the slice centers. When σ_o is found, it is necessary to report where the corresponding slice locations are on Earth's surface. In this manner the wind speed and direction can be mapped correctly. Tabularizing this computation dramatically speeds it up. However, as with the X factor, the slice centers are affected by perturbations. If the slice centers⁴ are incorrectly reported, then the wind data

³The nominal case includes the nominal orbit parameters, perfect attitude, and perfect Doppler and range tracking.

⁴The slice center locations are given in terms of the azimuth and elevation angle by the Xfactor location table. The azimuth and elevation angles are converted to latitude and longitude using geometry code at

Figure 4: Scatter plots of X and azimuth and elevation centers vs. Baseband Frequency Shift



will not be plotted on the correct location. In order to account for perturbations a technique is used similar to the technique dealing with perturbations for the X factor. The azimuth and elevation angles for the slice centers are plotted versus Δf . In the slice center case only a linear fit is necessary, as can be seen in Fig. 4 (b) and (c). This fit gives the equations

$$\Phi_c = \Phi_{bs} + A_\Phi + B_\Phi \cdot \Delta f \quad (9)$$

and

$$\Theta_c = \Theta_{bs} + A_\Theta + B_\Theta \cdot \Delta f \quad (10)$$

where Φ_{bs} and Θ_{bs} are the boresight azimuth and elevation angles, respectively. $A_{\Phi,\Theta}$ and $B_{\Phi,\Theta}$ are tabulated coefficients and Δf is the baseband frequency shift. In this manner the slice center location coefficients are tabularized before the launch of SeaWinds, decreasing the computational load of the processing.

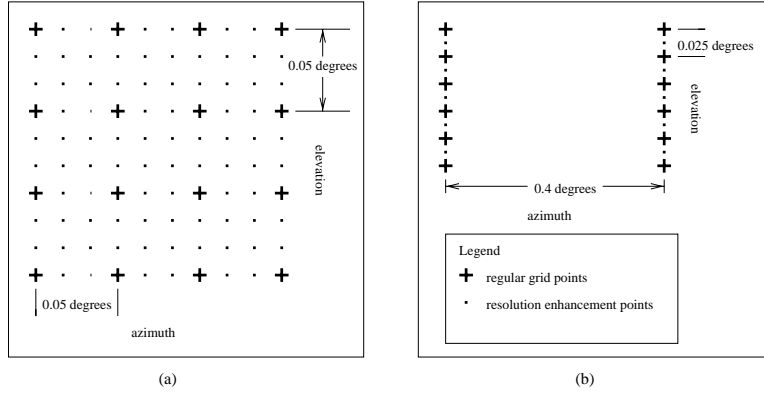
4 Accuracy Analysis of the Xfactor7 Table

4.1 Introduction

The Xfactor7 code is currently being used by JPL and BYU to produce the X Table. To calculate the integral of the X equation the response is summed up over the azimuth and elevation directions for each slice. To do this an integration grid is used. The size of the grid influences the size of errors and the time to generate the table. BYU has done extensive tests to quantify the accuracy of the Xfactor7 Table. In this section, the grid spacing is discussed, then the accuracy evaluation method, followed by an accuracy analysis of the Xfactor7 code, and finally an analysis of the calculation errors involved.

JPL.

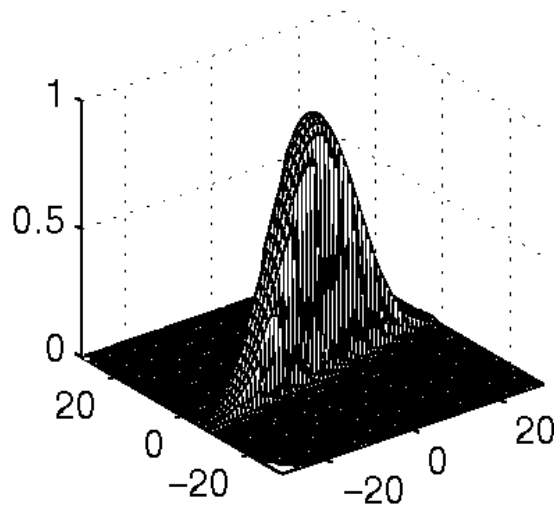
Figure 5: Square and Rectangular Spacing on an Integration Grid



4.2 Current Xfactor7 Grid Spacing

To generate X for a slice, the antenna gain and signal processing response is summed up over the azimuth and elevation directions. This requires a certain grid spacing to sum over. Generally, if the grid spacing is decreased the accuracy of X increases. The X Table initially was generated using a rectangular grid spacing over the azimuth and elevation angles as can be seen in Fig. 5 (a). But because of relative sharpness in some directions while smoothness in other directions (see Fig. 6), it made sense to change to a rectangular grid spacing (Fig. 5 (b)). This results in a dramatic decrease in the time to produce an X Table because the spacing is much larger in the azimuth direction. This can be done without a significant increase in errors for X or the slice center locations. The current recommended grid spacing for the inner beam is $\Delta\Phi=0.4$ and $\Delta\Theta=0.025$ for the azimuth and elevation directions, respectively. For the outer beam the recommended grid spacing is $\Delta\Phi=0.4$ and $\Delta\Theta=0.020$.

Figure 6: A typical slice response



4.3 Accuracy Analysis Method

Because the integral in Eq. (5) is evaluated as a discrete sum, the result is only an approximation. In order to quantify the errors in X and the slice center locations, an extensive test has been done on the Xfactor7 Table⁵. The test is conducted for 16 evenly spaced orbit times, with 100 random perturbations for each beam for each time. For each orbit time, a uniform distribution for the azimuth angle is used and a Gaussian random distribution is used for the perturbations. The perturbations are those expected for SeaWinds on QuikSCAT, namely, $\mu=0.0$ and $3\sigma= \pm 0.1$ for roll, pitch, and yaw, $\mu=90.0$ and $3\sigma=\pm 10.0$ for the argument of perigee, and $\mu=0.0012$ and $3\sigma=\pm 0.0002$ for eccentricity.

The test is conducted by generating the expected values of X , Δf , and the slice center locations in terms of Φ_c (azimuth angle) and Θ_c (elevation angle). These are generated for specific orbit times, azimuth angles, and perturbations⁶. Next, the coefficients for the X and the cell center location equations (see Eqs. 5, 10, and 11) are interpolated from the X Table for the same orbit times and azimuth angles in the same manner that will be done when SeaWinds is in orbit. Then X , Φ_c , and Θ_c are calculated manually by plugging in the interpolated coefficients and the generated Δf . The calculated values are then compared to the expected values to ascertain the accuracy of the Xfactor7 table.

4.4 Accuracy Results

The maximum errors for the inner slices⁷ are included in Table 1. The errors show that the outer beam is actually more accurate than the inner beam. A histogram of the errors for the inner slices is given in Fig. 7⁸. The errors for the outer slices are much greater than the inner slices because of fringe effects. The errors for the outer slices are plotted in Fig. 8⁹. The sum of all the inner slice responses constitutes the egg response, X_{egg} . X_{egg} errors for the inner and outer beams are found in Figures 9 and 10, respectively, and the maximum errors are in Table 1.

Table 1: Maximum error for X , X_{egg} , azimuth, and elevation (inner slices)

Maximum Error	X (dB)	X_{egg} (dB)	Azimuth (degrees)	Elevation (degrees)
inner beam	0.12	0.009	0.024	0.008
outer beam	0.05	0.012	0.018	0.0045

⁵This table was generated for mode 6 using $\Delta\Theta=0.025$ and $\Delta\Phi=0.4$, with resolution enhancement modes 2 and 1, respectively.

⁶This was done by using the single output option from the Xfactor7 table using mode 6, $\Delta\Theta=0.01$, and $\Delta\Phi=0.1$, with resolution enhancement modes 2 and 1, respectively. The accuracy of this computation is better than .002 dB.

⁷The inner slices for this report are defined as slice 3 through slice 10.

⁸the axes for the same parameter are the same, but differ from the other parameter's axes

⁹The axes for slices 2 and 11 and for slices 1 and 12 are the same for identical parameters. This is done for ease of comparison without losing any information in the graphs.

In order to further understand the error histograms, the mean and the standard deviation are calculated for all four parameters. The plots are found in Fig. 11 for X and X_{egg} , and in Fig. 12 for the slice centers. On some of the figures the mean and/or standard deviation is too large to show for the outer slices without compromising the scale for the inner slices. The standard deviation for X and the slice center locations are given for all slices in Table 2. As can be seen from the table, the standard deviation for X is below 0.025 dB for the inner slices and for both beams. The standard deviation for azimuth is below 0.0065 degrees and elevation is below 0.002 degrees for the inner slices and for both beams. This shows that the Xfactor7 table is very accurate.

Table 2: Standard deviation of X, azimuth, and elevation (mode 6)

Parameter	Slice: 1	2	3	4	5	6
X ib	0.0442	0.0444	0.0210	0.0086	0.0026	0.0039
X ob	0.0263	0.0140	0.0086	0.0048	0.0041	0.0053
Azimuth ib	0.1270	0.0177	0.0063	0.0048	0.0035	0.0028
Azimuth ob	0.0361	0.0040	0.0039	0.0049	0.0036	0.0029
Elevation ib	0.0622	0.0024	0.0014	0.0011	0.0008	0.0005
Elevation ob	0.0031	0.0009	0.0008	0.0007	0.0006	0.0004
Parameter	Slice: 7	8	9	10	11	12
X ib	0.0042	0.0022	0.0072	0.0194	0.0388	0.0437
X ob	0.0047	0.0041	0.0053	0.0105	0.0359	0.0792
Azimuth ib	0.0033	0.0044	0.0054	0.0056	0.0138	1.717
Azimuth ob	0.0032	0.0040	0.0041	0.0052	0.0025	0.6868
Elevation ib	0.0005	0.0008	0.0012	0.0017	0.0023	0.1994
Elevation ob	0.0004	0.0006	0.0007	0.0008	0.0023	0.1040

4.5 Calculation Error Analysis

The table accuracy is dependent on the grid spacing. If the grid spacing is large, the errors will also be large because of lost information due to the coarseness of the grid. To quantify calculation errors, X and the slice center locations¹⁰ are plotted in Figures 13, 14, and 15. Each mark¹¹ represents a different grid spacing with different resolution enhancement modes, the larger computation times occurring with the smaller grid spacings. As can be seen, the calculated values converge as the computation time increases. The calculation error is estimated as the difference between the value from the grid size used for testing (*) and the converged point. The plots show that the calculation error for the inner slices is approximately 0.002 dB for X , 0.0075 degrees for the azimuth angle, and 0.001 degrees for the elevation angle.

¹⁰normalized by the smallest value

¹¹The asterisk represents the same grid size and resolution enhancement mode used for the Xfactor7 table generated for testing.

5 Conclusion

In order to calculate the wind speed and velocity, σ_o must be processed for all slices for each antenna footprint. To accelerate real-time processing of σ_o for SeaWinds, the X factor and the slice center locations are tabularized pre-launch for the perturbations expected for SeaWinds on QuikSCAT. The test results show that this can be done without compromising accuracy. All errors for both beams are shown to be less than 0.12 dB for X , 0.012 dB for X_{egg} , 0.024 degrees for the azimuth angle, and 0.008 degrees for the elevation angle.

Figure 7: X , azimuth, and elevation errors for the inner slices

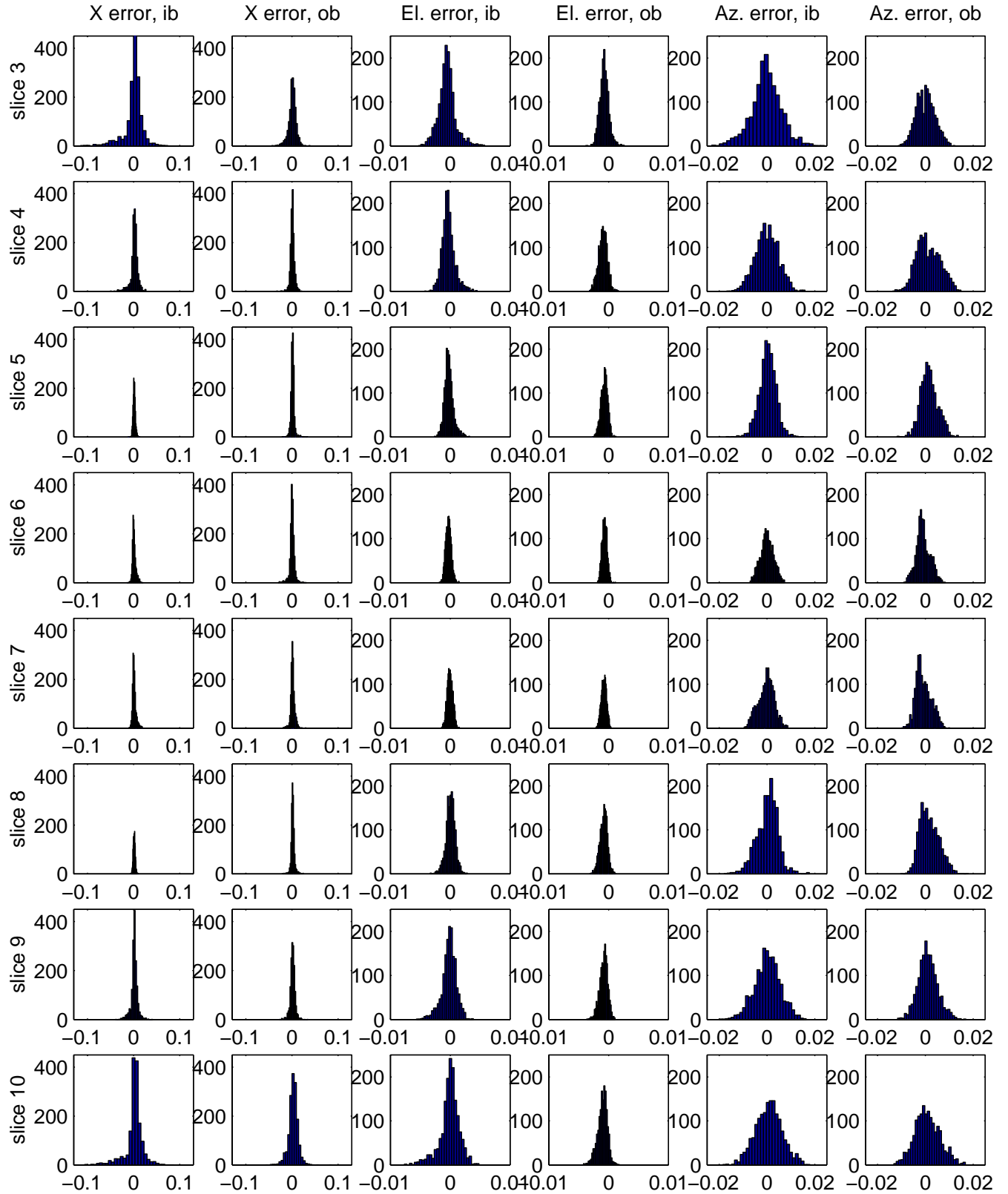


Figure 8: X , azimuth, and elevation errors for the outer slices

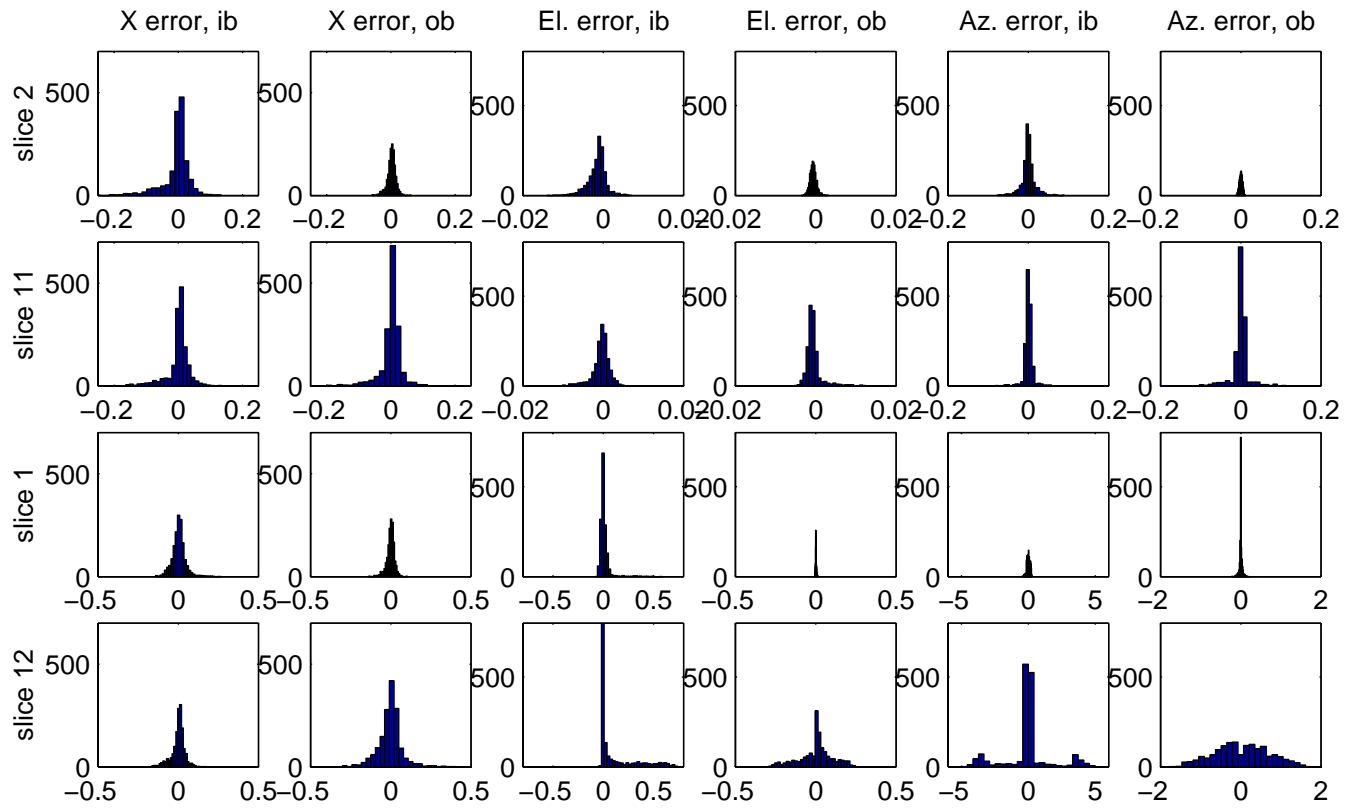


Figure 9: X error for the egg, inner beam (dB)

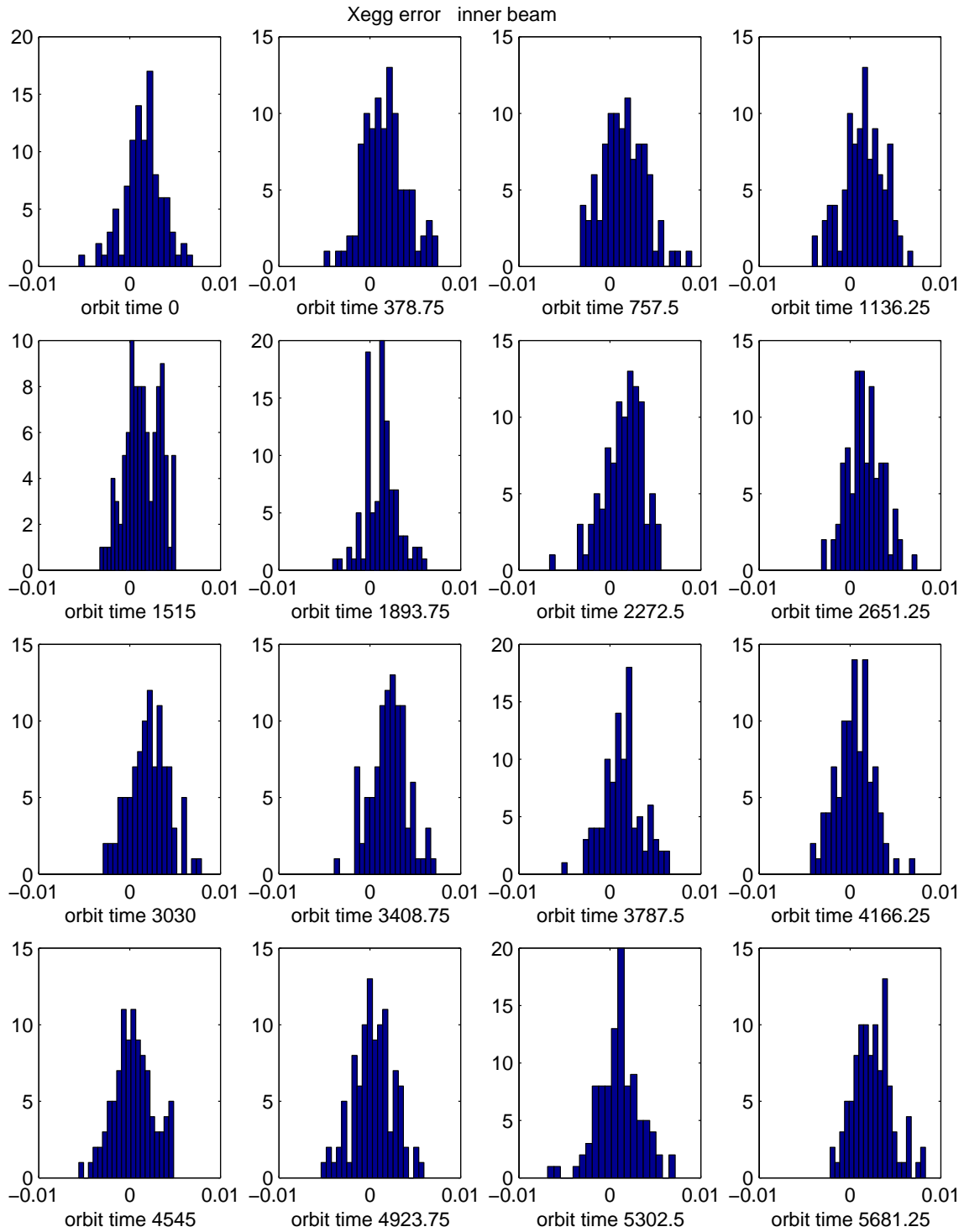


Figure 10: X error for the egg, outer beam (dB)

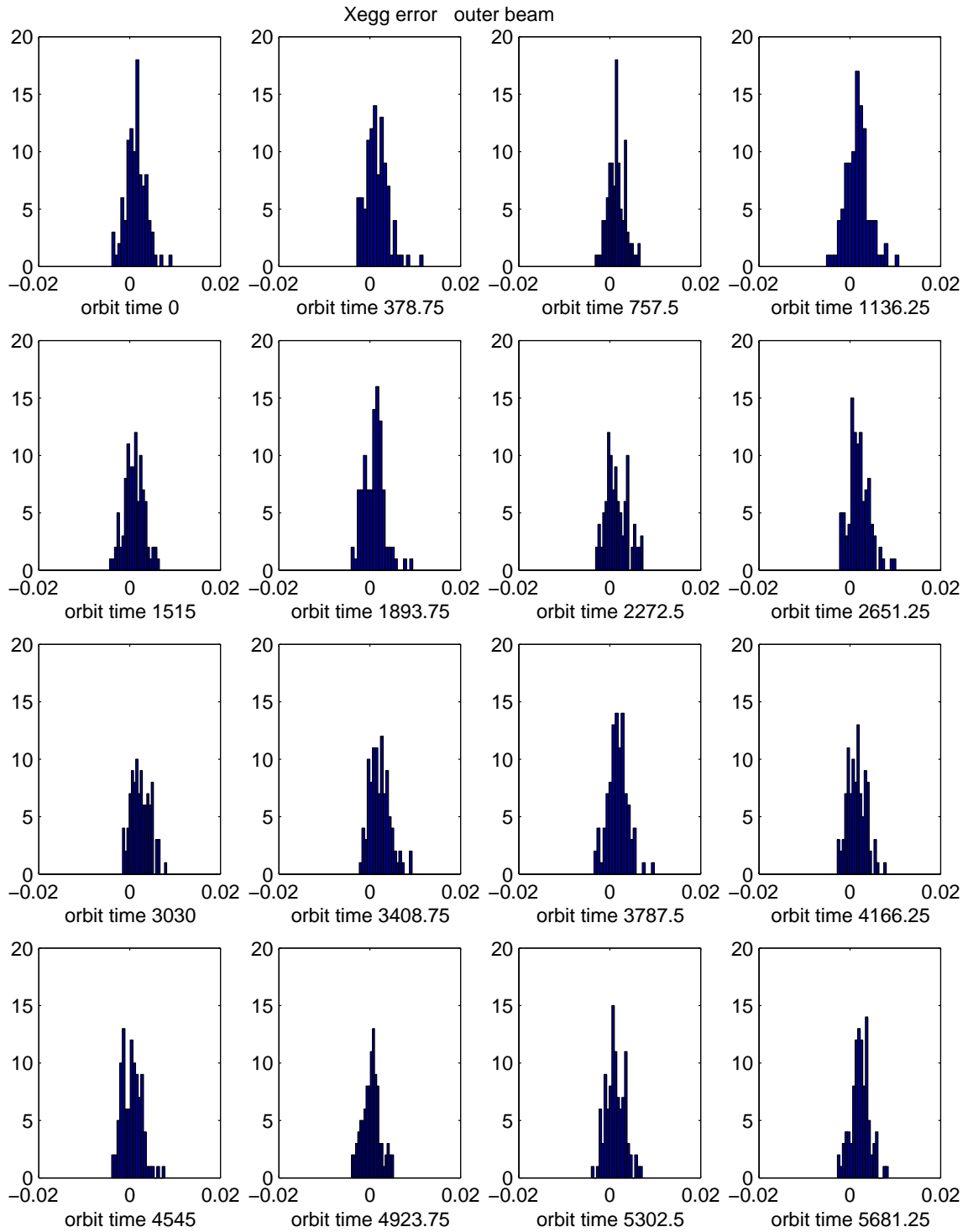


Figure 11: Mean and standard deviation for X and X_{egg} (dB)

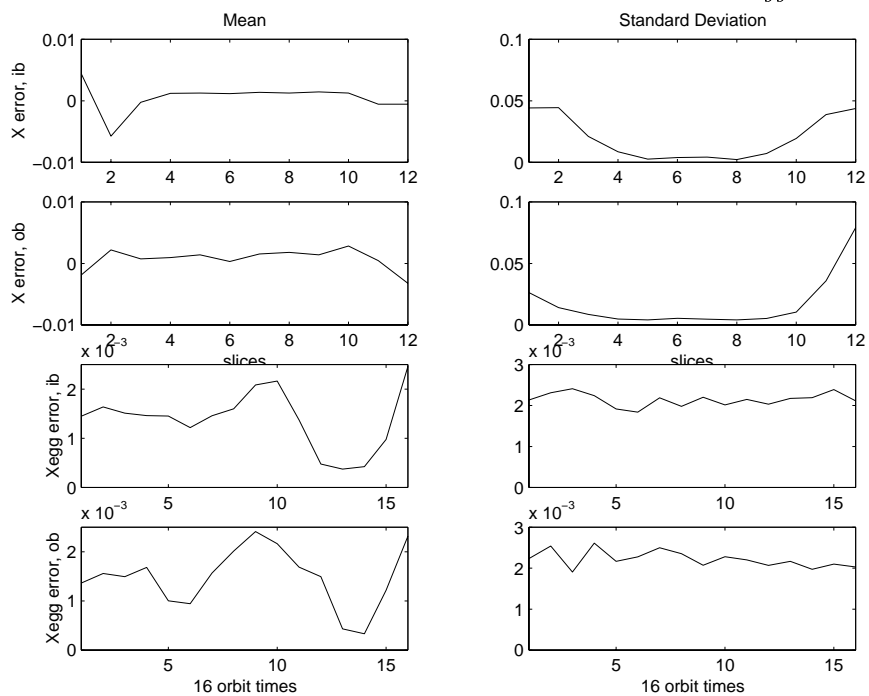


Figure 12: Mean and standard deviation for the slice centers (degrees)

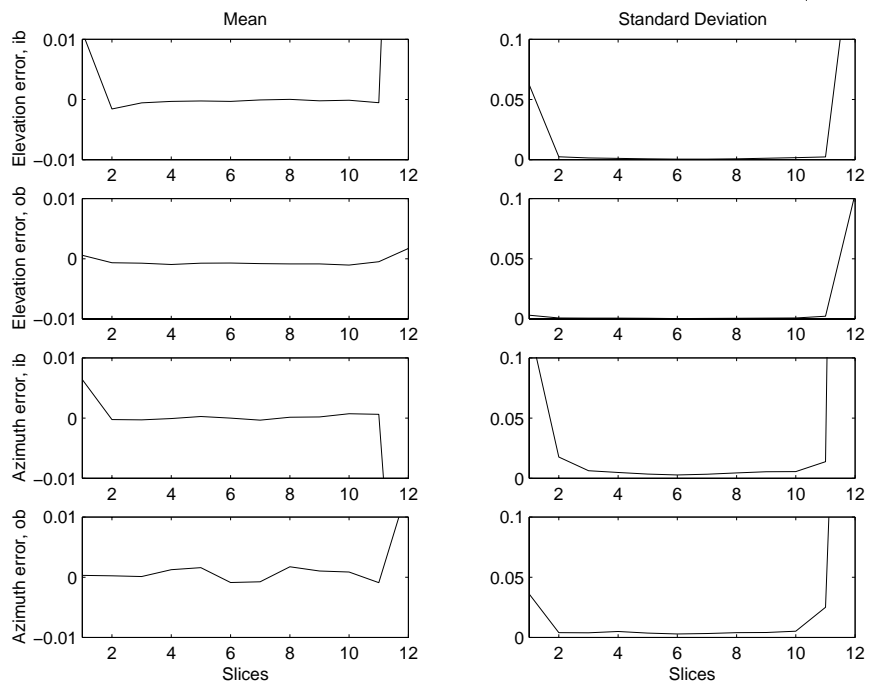


Figure 13: X versus computation time(dB)

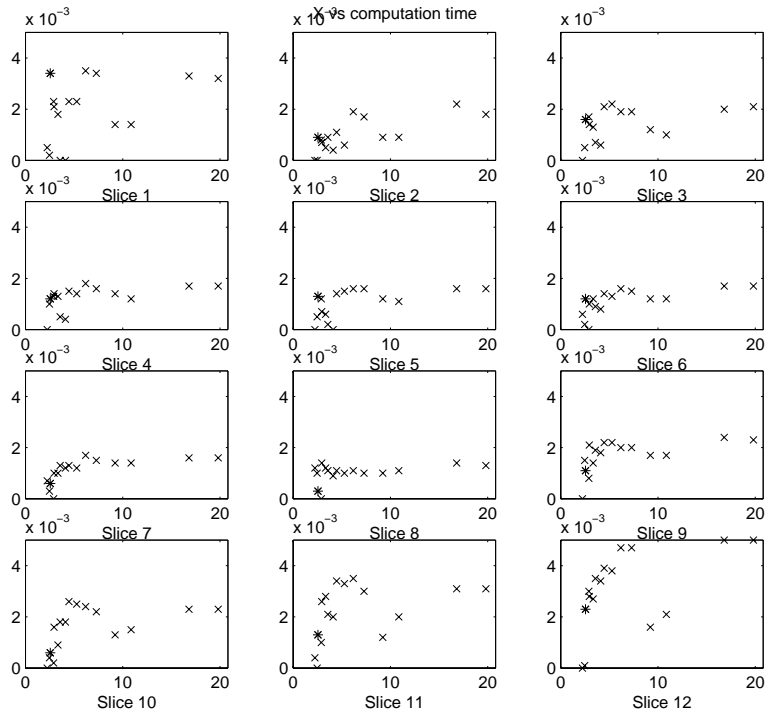


Figure 14: Azimuth angle versus computation time(degrees)

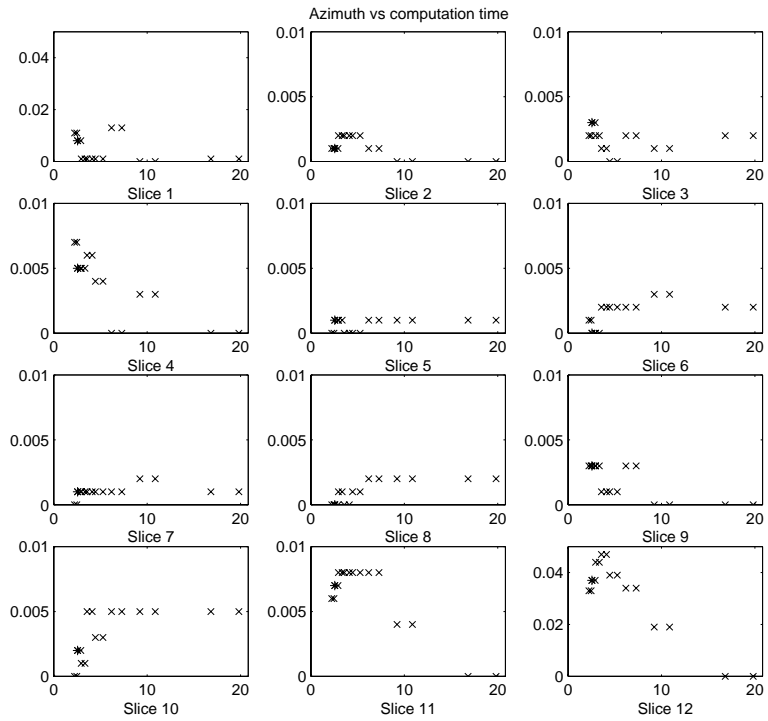


Figure 15: Elevation angle versus computation time(degrees)

